Peer-reviewed version available at Technologies 2017, 5, 82; doi:10.3390/technologies5040082

Article

Photodegradation of 1-butyl-3-methylimidazolium chloride [bmim]Cl via synergistic effect of adsorption-photodegradation of Fe-TiO_2/AC

Azhar Zawawi , Raihan Mahirah Ramli * and Noorfidza Yub Harun

Chemical Engineering Department, Universiti Teknologi PETRONAS, 32610, Bandar Seri Iskandar, Perak; azharz.utp@gmail.com, raihan.ramli@utp.edu.my, noorfidza.yub@utp.edu.my

* Correspondence: raihan.ramli@utp.edu.my; Tel.: +605 - 368 7553

Abstract: Ionic liquids (ILs) have gained interest among researchers due to its tunable properties that can be used in wide applications. However, toxicity and bio-degradation studies of ILs proved that most of the aromatic ILs, such as imidazolium is highly toxic and non-biodegradable. Several advance oxidation processes (AOPs) have been investigated by researchers to evaluate the efficiency of the systems for the removal of ILs from wastewater. However, the issue on relative high cost and environmental concern has limited the application of these AOPs in industry. In this research, photocatalytic study using hybrid nano-materials was conducted to evaluate the efficiency of this system as an alternative AOP system for removal of ILs from wastewater. The synergistic effect of adsorption-photodegradation was introduced by depositing Fe-TiO_2 onto the functionalized activated carbon (AC). Nano-TiO_2 was synthesized using micromulsion method before modification with transition metal and deposited onto the oxidized AC. Photodegradation reaction of 1-butyl-3-methylimidazolium chloride [bmim]Cl was investigated under simulated visible light irradiation. It was observed that the overall efficiency of the system was increased with the increasing amount of Fe dopant. Investigation on the extrinsic factors such as solution pH, initial concentration of ILs and photocatalyst dosage showed to significantly affect the overall efficiency of the systems where the optimum condition for the system was observed at pH 10, with initial ILs at 1mM at 1 g/L of photocatalyst. The best performance photocatalyst was 0.2Fe-TiO_2/AC.

Keywords: photodegradation; TiO_2; ionic liquids; activated carbon; synergistic effect

1. Introduction

Ionic liquids (ILs) is a chemicals that can be synthesized either via metathetic exchange of anion, neutralization with Brønsted acid, direct alkylation and alkylimidazole or carbonate route [1]. Depending on its specific applications, the physical and chemical properties of ILs are tunable by varying its cation and anion. ILs is currently being used in industry for both large scale production and pilot plant study. For instance, PETRONAS has applied ILs for mercury removal process while BASF and Institutes Francis de Petrole Axens (IFP) have employed ILs in biphasic acid scavenging ionic liquids (BASIL) PROCESS and dimersol process, respectively [2].

The increasing number of ILs applications has raised the concern towards the impact of ILs to the environmental due to its high solubility and persistence in water. Biodegradation studies on ILs which was conducted by a few researchers have concluded that ILs with aromatic ring cation such as imidazolium is non-biodegradable [3-5]. On the other hand, this type of IL has been widely used in bio industry [1]. Hence, efficient treatment system that is able to overcome the high solubility properties of ILs in water is urgently required. Advance oxidation process (AOP) is widely known for its efficient for degradation of wide range of organic pollutants [6]. Photocatalytic degradation employing semiconductor as the photocatalyst is one of the AOP that is efficient to treat ILs in wastewater [7]. This process can be considered as relatively low cost and sustainable since it is able to harvest solar energy into chemical reaction [8].

Among the semiconductor available for the application, titania (TiO_2) is the most researched semiconductor used as photocatalyst [9]. The major drawback of TiO_2 that hinders its application in industry as photocatalyst, however, is the limited range of light absorption in UV region only. In addition, TiO_2 has a comparatively slow diffusion rate between the target pollutant and its surface [10, 11]. These limitations could be overcome through modification of the TiO_2 via several methods such as doping with metals, depositing TiO_2 onto AC as support and doping another semiconductor onto TiO_2 as co-catalyst. The introduction of metal dopants onto TiO_2 has significant enhanced its activity under visible light, thus improving its overall performance of the system [9]. The modification process causes defect to the TiO_2 structure such as oxygen vacancy (V_o) and Ti^{3+} leading to the reduction of band gap energy. Hence, absorbance of TiO_2 is shifted towards the visible light region [12].

Furthermore, addition of activated carbon to TiO_2 has a dual function; as a support and at the same time as the center of accumulation for the pollutant. The presences of hydroxyl groups (OH) on AC surface are able to attract [bmim]Cl towards the surface of the photocatalyst thus enhance the diffusion rate of [bmim]Cl into TiO_2. The synergistic effect of adsorption-photodegradation of composite photocatalyst has consequently increased the overall efficiency of the system [13]. Apart from intrinsic factors, the extrinsic factors such as initial ILs concentration, initial pH of ILs solution and photocatalyst dosage has been reported to have significant effect to the overall efficiency of the systems [14].

In this paper, the work is focused on the development of hybrid nano-photocatalyst consisting of nano-TiO_2 synthesized via microemulsion method followed by modification with Fe and deposited on AC surface. The efficiency of the developed photocatalyst was evaluated in a photocatalytic degradation system containing [bmim]Cl solution at the desired concentration under 500W visible light energy source. Several parameters that were reported to be highly significant to the photodegradation process will be investigated.

.

2. Materials and Methods

2.1. Materials

All chemicals were purchased and used without further purification. Hexanol ($C_6H_{14}O$, 98%), ferum nitrate nonahydrate ($Fe.(NO_3)_3.9H_2O$), 1-butyl-3-methylimidazolium chloride, [bmim]Cl ($C_8H_{15}ClN_2$), heptane (C_7H_{16}, 99%), Ethanol (C_2H_3OH, 95%) and titanium tetraisopropxide, TTIP ($C_{12}H_{28}O_4T$, 97%) were purchased from Merck (Germany). Meanwhile other chemicals such as nitric acid (HNO_3, 65%), triton X-100 ($C_{34}H_{62}O_{11}$, AR), potassium dihydrogen phosphate (KH_2PO_4) and triethylamine ($C_6H_{15}N$, AR) were supplied by R&M Chemicals (Malaysia) and phosphoric acid (H_3PO_4, 85%) was purchased from QreC (New Zealand).

2.2. Methods

Nano-TiO_2 was synthesized using water-in-oil microemulsion method as reported from previous study [7] followed by modification with the desired Fe via wetness impregnation method. The resultant powder from the impregnation method was calcined at 400 °C for 1.5 h. In a different set up, the pre-carbonized AC was oxidized using 1M of nitric acid in a boiling condition for 20 minutes. The oxidized AC was washed repeatedly with distilled water until the filtrate became neutral. The oxidized AC was then dried overnight in an oven at 80 °C. Finally, the developed, Fe-TiO_2 and AC were mixed (10 wt% AC) using impregnation method as reported in our previous study [15]. The final photocatalyst was denoted as *a*Fe where *a* refer to amount of Fe dopant ie; 0.2Fe refer to 0.2 wt% Fe deposited onto TiO_2/AC.

2.3. Characterization Photocatalyst

Characterization of the photocatalyst was conducted to analyze its physical and chemical properties. The effect of adding AC to the photocatalyst surface was evaluated by analyzing the

existing functional group using Fourier Transform Infrared (FTIR). The analysis was conducted using Shimadzu FTIR-8400S Spectrophotometer. Absorbance and band gap of the photocatalyst was conducted using UV-Visible Spectroscopy. An optical property of the photocatalyst was conducted using Agilent Technologies Cary 100 UV-Vis Spectrophotometer Model G9821A. The pH_{PZC} of the photocatalyst was employed using mass titration method as reported from previous study [16].

2.3. Photodegradation Study

The performance of the developed photocatalyst was evaluated in the photocatalytic degradation of [bmim]Cl using open glass reactor in ambient conditions. In a typical experiment work, a pre-determined amount of photocatalyst was added into the reactor containing desired concentration of [bmim]Cl solution. The system was stirred in dark for 30 mins to allow for equilibrium adsorption-desorption process, followed by 2 h irradiation under 500 W halogen lamp. Liquid samples were collected at regular time intervals and analyzed using high performance liquid chromatography (Agilent 1100 HPLC). For better separation and sharp analysis, column symmetry C-18 (250 x 4.6 mm, 5 µm) and mobile phase mixture of methanol (35 vol%) and 25 mM of phosphate buffer (KH_2PO_4/H_3PO_4) containing 0.5 % of triethylamine were used. The analysis was performed at 30 °C column temperature, 5 µL sample injection and 0.8ml/min flow rate. The separated [bmim]Cl was detected at 212 nm wavelength using UV detector.

3. Results

3.1. Characterization of the photocatalyst

3.1.1 Fourier Transform Infrared (FTIR)

Figure 1 shows the vibration peak of different photocatalysts with respect to Fe content.

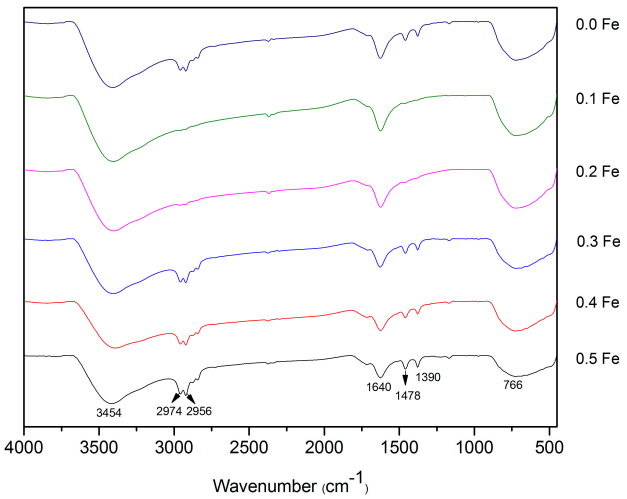

Figure 1. FTIR spectra of photocatalyst at different amount of Fe

3.1.2. Optical Property (UV-Vis)

The absorption spectra of the photocatalyst at different amount of Fe are presented in Figure 2.

Preprints (www.preprints.org) | NOT PEER-REVIEWED | Posted: 24 October 2017 doi:10.20944/preprints201710.0159.v1

Peer-reviewed version available at Technologies 2017, 5, 82; doi:10.3390/technologies5040082

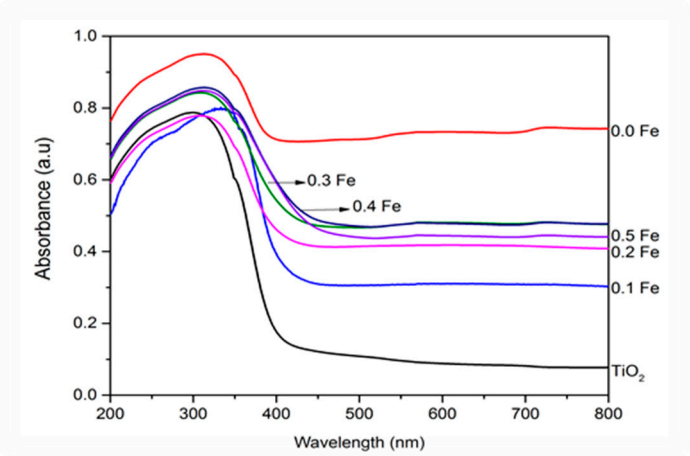

Figure 2. Absorption spectra of the photocatalyst

The TiO_2 band gap energy was estimated from the extrapolation of tauc plot and tabulated in Table 1. As a control, the synthesized TiO_2 has been treated in similar procedure as for the preparation of TiO_2/AC and Fe-TiO_2/AC. Similar procedure steps were also taken to P25 to ensure comparable data analysis.

Table 1. Band gap energy of photocatalyst

Photocatalyst	Band gap energy (ev)
P 25	2.80
TiO_2	2.77
0.0 Fe	2.57
0.1 Fe	2.58
0.2 Fe	2.35
0.3 Fe	2.17
0.4 Fe	2.06
0.5 Fe	2.03

3.1.3. Surface Charge (pH_{pzc})

Point zero charge (pH_{PZC}) of photocatalyst can be defined as the limiting pH when the net surface charge of photocatalyst is zero. The pH_{pzc} study of photocatalyst was determined using titration method as reported from previous study [16].

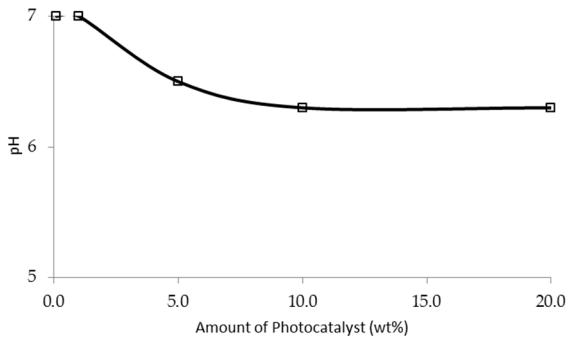

Figure 3. Surface charge of photocatalyst for 0.2Fe-TiO_2/AC

Peer-reviewed version available at Technologies 2017, 5, 82; doi:10.3390/technologies5040082

3.2.Photodegradation Study of [bmim]Cl

The photodegradation analysis of [bmim]Cl was optimized by using one factor at a time experiment (OFAT) analysis. Factors such as composition of dopants, initial concentration of [bmim]Cl [IL_o], initial pH of solution and photocatalyst dosage were investigated to study the effect of the parameters in degradation of [bmim]Cl.

3.2.1. Effect of Fe Composition

The effect of Fe loading to the degradation efficiency of [bmim]Cl is depicted in figure 4. The percentage of degradation increased as the amount of dopant increase.

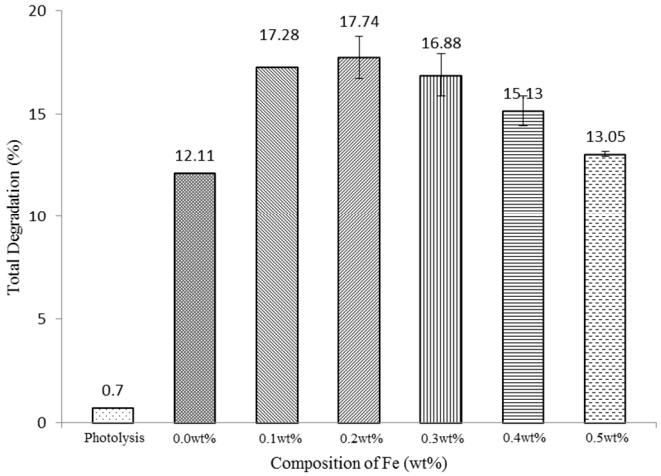

Figure 4. Efficiency [bmim]Cl degradation system for different amount of Fe at [IL_o] = 5 mM, pH = 8 and [photocatalyst] = 1 g/L.

3.2.2. Effectof Extrinsic Factor: Initial Concentration of [bmim]Cl (IL_o)

Peer-reviewed version available at Technologies 2017, 5, 82; doi:10.3390/technologies5040082

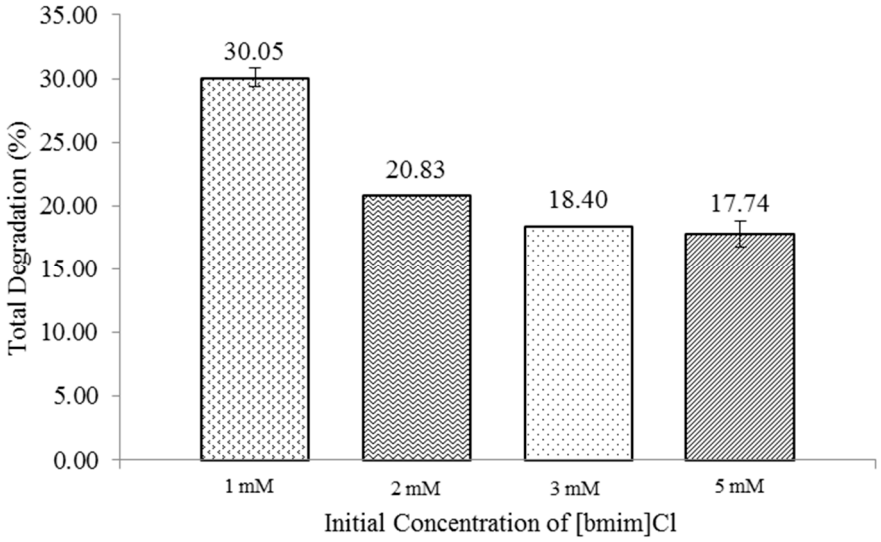

Figure 5. Efficiency of [bmim]Cl degradation system at different [IL$_o$]

Figure 5 present the effect of initial concentration of [bmim]Cl [IL$_o$] to the overall performance of the system. The study was conducted by keeping other parameters constant i.e 0.2 wt% Fe, pH 8 and 1 g/L of photocatalyst. As the [IL$_o$] was reduced, the total percentage degradation recorded increased.

3.2.3. Effect of Extrinsic Factor: pH of [bmim]Cl solution

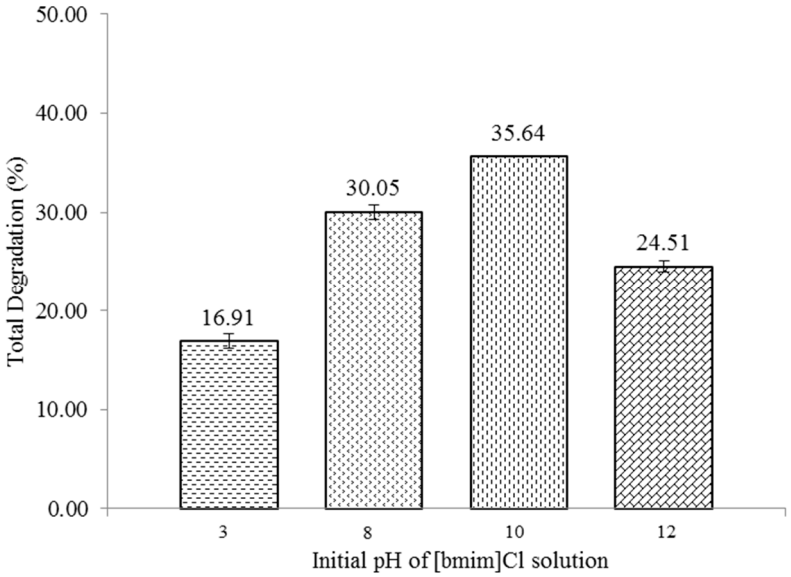

Figure 6. Efficiency of [bmim]Cl degradation system at different initial pH of [bmim]Cl solution

Pursuant to section 3.2.2, optimum [IL$_o$] was observed at 1 mM. Hence, this [IL$_o$] has been selected to study the effect of initital pH of [bmim]Cl solution while keeping other parameters constant i.e 0.2 wt%Fe, [IL$_o$] at 1 mM and 1 g/L of photocatalyst. Figure 6 depicts the comparative study pH of [bmim]Cl solution. As the initial solution pH increased, the total removal of [bmim]Cl increased up to the optimum point, then decreased.

Peer-reviewed version available at Technologies 2017, 5, 82; doi:10.3390/technologies5040082

3.2.4. Effect of Extrinsic Factor: Dosage of Photocatalyst

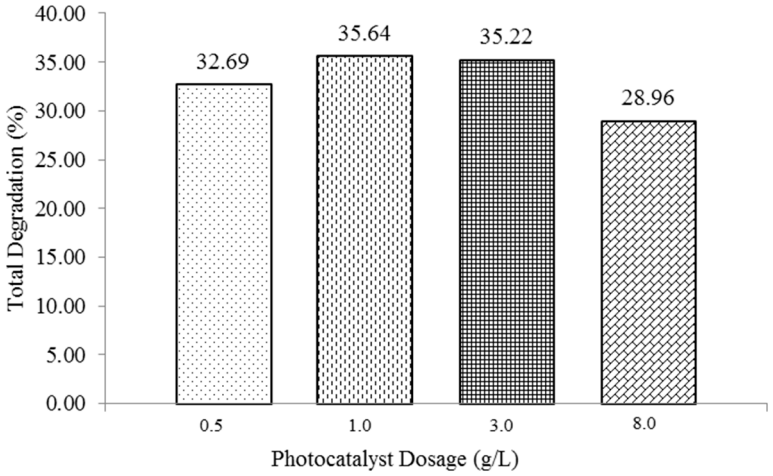

Figure 7. Efficiency of [bmim]Cl degradation system at different [photocatalyst]

The effect of photocatalyst dosage, [photocatalyst] to the effeciency of the system was evaluated by keeping other factors constant i.e 0.2 wt% Fe, [IL_o] at 1 mM and initial pH 10. Figure 7 summarizes the removal efficiency at different [photocatalyst]. as can be observed from the figure, [photocatalyst] has significant effect to the total removal of [bmim]Cl.

4. Discussion

4.1 Fourier Transform Infrared (FTIR)

From Figure 1, the first broader peak recorded at at 766 cm^{-1}, could be ascribed to the titania framework that has been deposited onto AC such as Ti—O—Ti [13, 17, 18]. The vibration peak recorded at 1390 cm^{-1} represent the C=O stretching related to carboxylic groups and carboxylate moieties [19, 20] while the presence of C=O stretching could be due to the oxidation treatment of AC with nitric acid. The usage of acid as treatment agent was also stated that it could produce homogenous distribution of titania with complex structure [19]. This can be supported with vibration peak around 766 cm^{-1} which shows strong vibration of Ti—O proving that TiO_2 is well distributed on the surface of AC [21].

The small and sharp vibration peaks of C-H have been detected in IR spectra at wavenumber 1390 and 1478 cm^{-1}. These peaks show that the dissociation of precursor TiO_2/AC may occur leaving behind the substrate such as O, Ti and C. The presence of C—H bond is also stated to be chemisorbed [22]. Meanwhile, peak at 1640 cm^{-1} represents the vibration of O—H that may comes from adsorption of H_2O onto surface of photocatalyst [13, 21, 22]. Small peak detected at 2412 cm^{-1} represents the double bond that may present on surface of photocatalyst such as C=O [22]. Two close vibration peaks at 2956 and 2974 cm^{-1} also represent the O—H stretching. Broader peak at 3454 cm^{-1} represent the O-H group [13, 21, 22]. The presence of this broader peak shows high vibration of O-H that exist on AC's surface that has been oxidized with nitric acid. This is in line with the purpose of oxidation treatment which is to obtain more hydrophilic surface of photocatalyst with oxygen-containing functionalize group on surface of AC such as O—H group [19]. In adsorption study of hydrophobic ILs, the presence of O—H is important as it could act as pollutant concentrator for the composite photocatalyst. The O—H group that present on the surface of photocatalyst were able to promote the H-bonding interactions with anion of hydrophobic ILs [23, 24].

4.2. Oprical Property (UV-Vis)

Significant shift of the absorbance edge at 400 nm wavelength could be observed for all photocatalysts containing Fe. This shift could be ascribed to the excitement of electron (e^-_{CB}) from valence band (VB) of TiO_2 as describe by equation (1-3) [25]. The h^+_{VB} and trapped electron (*et*) refer to hole form at VB after excitement of e^-_{CB} and electron that has been trapped on surface AC and dopant respectively.

$$TiO_2 + hv \rightarrow TiO_2\,(e^-_{CB}) + TiO_2\,(h^+_{VB}) \quad (1)$$

$$TiO_2\,(h^+_{VB}) \xrightarrow{organic\ groups} TiO_2 \quad (2)$$

$$TiO_2\,(e^-_{CB}) \rightarrow TiO_2\,(et) \quad (3)$$

The h^+_{VB} will then be scavenged through interaction with organic groups that is present on AC surface which led to the formation of new trapped electron. This continuous phenomenon creates centers of excitons which then will cause the red shift and additional peak of the absorption onset [25]. The trapped electron could also occur from e^-_{CB} to dopant on photocatalyst before the *et* be excited again to the TiO_2 surface to undergo redox process as per equation (4-7). The e^- refer to electron from dopant itself.

$$Fe^{3+} + TiO_2\,(e^-_{CB}) \rightarrow Fe^{2+} \quad (4)$$

$$Fe^{2+} \rightarrow Fe^{3+} + TiO_2(et) \quad (5)$$

$$Fe^{3+} \rightarrow Fe^{4+} + e^- \quad (6)$$

$$Fe^{4+} + TiO_2(et) \rightarrow Fe^{3+} \quad (7)$$

From Table 1, the estimated band gap energy of TiO_2 and P25 were approximately lower than reported [26] which could be due to the treatment procedure. It could be deduced that this reduction occurred due to: 1) when P25 and TiO_2 were calcined after the impregnation processes, the phase structure of photocatalyst increased hence reducing the band gap energy as reported from previous study [26, 27] and 2) transformation of anatase to rutile could occur which led to reduction in band gap energy [26, 28]. The band gap of TiO_2 doped with Fe also shows significant reduction with the increased amount of Fe (Table 1). This phenomenon could be explained when the excited e^-_{CB} combine with Fe dopant as the mid band gap energy introduced by dopant is low compared to band gap of bare TiO_2. Then, the e^-_{CB} can be excited again from dopant to CB of TiO_2. The reduction in band gap energy mean that the photocatalyst requires lower energy to generate more charge carrier to undergo redox process for degradation of [bmim]Cl [7].

4.3Surface Charge (pH_{pzc})

It was found that, the pH_{pzc} of photocatalyst was 6.3 (Figure 3). On the other hand, the pH of [bmim]Cl solution was recorded around 8.2 $\pm$ 0.2 regardless of [bmim]Cl concentration. Generally, when the pH of the solution is higher than pH_{pzc} of photocatalyst, the surface of photocatalyst will be negatively charged. Different charges between the photocatalyst surface and its [bmim]Cl will attract each other, hence increase the diffusion rate of [bmim]Cl into TiO_2 [9].On the other hand, similar charges between both entities reduce the ability for TiO_2 to attract [bmim]Cl compound towards its surface.

4.4. Effect of Fe Composition

Positive effect of increasing Fe amount could be observed in Figure 4. This is because, as the amount of Fe dopant increased, the band gap energy of TiO_2 decrease as proven in tauc plot analysis

(Table 1). Consequently, lower energy is required to initiate the generation of charge carrier to proceed with redox process and consequently degrade [bmim]Cl compound. In theory, upon radiation of light energy at certain value, e_{CB}^- could be excited to the covalence band of TiO_2 (CB). These electrons will be trapped by metallic dopant Fe^{3+} with the value of redox potential 0.77 eV respect to flat band potential (V_{fb}) of TiO_2 and follow several redox reaction as in equation (4-7) [12].

Based on the classical field theory, the formation of Fe^{2+} and Fe^{4+} is very unstable. This is because in their molecular state $3d^5$ configuration, it is only occupied with half-filled electron. Hence, the charge carrier can be migrated to the surface of TiO_2 to degrade the [bmim]Cl. The Fe^{2+} can be returned back to Fe^{3+} by donating one (e_{CB}^-) either directly to [bmim]Cl or to H_2O to undergo reduction process. H_2O will be reduced to form strong radical such as hydroxyl radical ($OH^\bullet$). These radicals are active species that could attack wide range of organic pollutants thus enhance the degradation rate of pollutants. Meanwhile Fe^{4+} can be transformed to Fe^{3+} by receiving an electron or lose a hole (h_{VB}^+). The (h_{VB}^+) will come in contact with the oxygen (O_2) that also has been adsorbed on surface of TiO_2 leading to the formation of superoxide radical ($0_2^{-\bullet}$) [12, 29]. During the degradation process of [bmim]Cl, the formed($0_2^{-\bullet}$) will attack the C2, C4 and C5 of imidazolium ring and produce unstable by-product known as 1-alkyl-3-methyl-2,4,5-trioxoimidazolidine. The formation of these by-products means the first stage of the degradation process where the phenomenon opening ring of cation occurred [30].

However, when the amount of Fe dopant exceeds the optimum, the overall efficiency of the system was significantly reduced. Even though higher amount of Fe further reduced the band gap energy of TiO_2 (Table 1), it also acts as the recombination center for the charge carriers. Furthermore, formation of ferum oxide (Fe_2O_3) on surface of photocatalyst during the synthesis process not only enhanced the system's efficiency, excess amount of Fe_2O_3 will lead to the blockage of TiO_2 surface from harvesting the radiated light energy for chemical reaction. Hence, less charge carrier could be generated [29] leading to a reduced overall efficiency. The formation of oxygenated group on the surface of composite photocatalyst as proven by the IR spectra spectra (Figure 1) also plays an important role in the degradation of [bmim]Cl. The presence of functionalized groups such as O-H and –COOH is believed to able to increase the interaction of H-bonding between the surface of composite photocatalyst and the anion Cl^-. Hence more [bmim]Cl will be attracted to the AC on the surface which then enhance the diffusion rate between [bmim]Cl and surface TiO_2 resulting in the significant increase of the total removal of [bmim]Cl [24].

4.2. Effect of Extrinsic Factor: Initial Concentration of [bmim]Cl (IL_o)

In Figure 5, it can be observed that the total degradation of [bmim]Cl decreased with the increasing of [IL_o]. As the amount of [bmim]Cl in the solution increase, the number of [bmim]Cl molecule increased and leading to poor adsorption and degradation rate of pollutant. On the other hand, at lower [IL_o], the accumulation of the pollutant on surface of TiO_2 reduced providing more active surface area to absorb photon and generate the charge carrier. As more charge carriers been generated, more [bmim]Cl can be degraded. This phenomenon follows the Lambert law where as concentration of organic molecules reduced, it will increase the path length taken by the photon to enter the solutions [31].

4.3. Effect of Extrinsic Factor: Initial pH of [bmim]Cl solution

The effect of varying initial pH of [bmim]Cl solution during the photodegradation process can be observed in Figure 6. The lowest [bmim]Cl degradation was recorded in acidic region at pH 3. In acidic region, the surface charges of photocatalyst and organic molecule were both protonated. Similar charges between both species make them repel each other causing less adsorbate to be adsorbed onto the surface of photocatalyst. Further, causing lower amount of [bmim]Cl being degraded by the charge carrier [32]. In addition, the photocatalyst was reported to be agglomerated in acidic condition thus reducing the availability of TiO_2 active site that can be used to absorb photon

and adsorb [bmim]Cl [33]. From the study, the best working pH for photodegradation of [bmim]Cl was recorded in alkaline condition at pH 10. In this condition, the OH^- interacted with h^+_{VB} lading to higher production of $OH^\bullet$ thus increased the degradation rate of [bmim]Cl. However, at even higher alkalinity, both organic molecule and surface of the photocatalyst were deprotonated. Similar charges of both species again repelled each other causing less [bmim]Cl been adsorbed on the surface of TiO_2 hence reduced the total degradation **[32]**. This ionization of the surface charge photocatalyst in various pH conditions could be explained as in equation (8-9) [34].

$$TiOH + H^+ \rightarrow TIOH_2{}^+ \quad (8)$$

$$TiOH + OH^- \rightarrow TiO^- + H_2O \quad (9)$$

4.4. Effect of Extrinsic Factor: Dosage of Photocatalyst [photocatalyst]

The effect of photocatalyst dosage, [photocatalyst] on the overall efficiency of photodegradation system of [bmim]Cl was studied by varying the [photocatalyst] between 0.0 to 8 g/L. From Figure 7, the total degradation of [bmim]Cl increased until the optimum [photocatalyst] was achieved. Insufficient amount of photocatalyst supplied to the system will cause blockage of the active site by [bmim]Cl hence poor efficiency of the system [35]. As the dosage increased, the active site available for photodegradation process increased leading to higher degradation rate. Beyond the optimum dosage (1 g/L), the overall efficiency of the system decreased despite larger amount of photocatalyst being used in the system. High amount of photocatalyst in the system lead the screening phenomenon of particles which will causes blockage of active site of photocatalyst. Furthermore, excess photocatalyst also lead to the agglomeration of the nanoparticles that will reduce the total surface area of photocatalyst. Hence less photon will be absorb and reduce the formation of generation charge carrier [36].

5. Conclusions

From the analysis study of composition Fe dope onto TiO_2, it can be conclude that by doping metal with optimum amount on surface of TiO_2, it can shift the performance of TiO_2 into visible region and increase the performance of photocatalyst for removal of [bmim]Cl. By considering the effect of [IL_o], this factor highly influence the overall efficiency of the system. As excess [IL_o] was used, it will block the surface of TiO_2 from harvesting the light. The pH synthetic of waste water also affect the overall efficiency of the systems where the most optimum pH conditions was recorded at pH 10. At this condition, the available OH^- will increase the production of $OH^\bullet$ as attacking agent that will increase the total degradation of bmimCl. Lastly, optimum dosage of Fe-TiO_2/AC was recorded with 1 g/L as excess of photocatalyst will agglomerate and reduce the availability of active site of photocatalyst.

Acknowledgments: Special thanks to Universiti Teknologi PETRONAS (UTP) for funding from I-Gen Grant (IGEN 0153 DA-162) and Centralize Analytical Laboratory (CAL), UTP for the characterization analysis.

Author Contributions "A. Zawawi and R. M. Ramli conceived and designed the experiments; A. Zawawi performed the experiments; A. Zawawi and R. M. Ramli and N. Y. Harun analyzed the data; R. M. Ramli and N. Y. Harun contributed reagents/materials/analysis tools; A. Zawawi wrote the paper."

Conflicts of Interest: "The founding sponsors had no role in the design of the study; in the collection, analyses, or interpretation of data; in the writing of the manuscript, and in the decision to publish the results".

References

[1] H. Olivier-Bourbigou, L. Magna, and D. Morvan, "Ionic liquids and catalysis: Recent progress from knowledge to applications," *Applied Catalysis A: General*, vol. 373, pp. 1-56, 2010.

[2] N. V. Plechkova and K. R. Seddon, "Applications of ionic liquids in the chemical industry," *Chem Soc Rev*, vol. 37, pp. 123-50, Jan 2008.

[3] E. M. Siedlecka, A. Fabiańska, S. Stolte, A. Nienstedt, T. Ossowski, P. Stepnowski, *et al.*, "Electrocatalytic Oxidation of 1-Butyl-3-Methylimidazolium Chloride: Effect of the Electrode Material," *International Journal of ELECTROCHEMICAL Science*, pp. 5560 - 5574, 2013.

[4] M. Munoz, C. M. Domínguez, Z. M. de Pedro, A. Quintanilla, J. A. Casas, and J. J. Rodriguez, "Ionic liquids breakdown by Fenton oxidation," *Catalysis Today*, vol. 240, pp. 16-21, 2015.

[5] H. Zhou, Y. Shen, P. Lv, J. Wang, and P. Li, "Degradation pathway and kinetics of 1-alkyl-3-methylimidazolium bromides oxidation in an ultrasonic nanoscale zero-valent iron/hydrogen peroxide system," *Journal of Hazardous Material*, vol. 284, pp. 241-52, Mar 02 2015.

[6] A. Buthiyappan, A. R. Abdul Aziz, and W. M. A. Wan Daud, "Recent advances and prospects of catalytic advanced oxidation process in treating textile effluents," *Reviews in Chemical Engineering*, vol. 32, pp. 1-47, 2016.

[7] R. M. Ramli, F. K. Chong, and A. A. Omar, "Visible-Light Photodegradation of Diisopropanolamine Using Bimetallic Cu-Fe/TiO_2 Photocatalyst," *Advanced Materials Research*, vol. 845, pp. 421-425, 2013.

[8] R. M. Ramli, C. F. Kait, and A. A. Omar, "Remediation of DIPA contaminated wastewater using visible light active bimetallic Cu-Fe/TiO_2 Photocatalyst," *Procedia Engineering*, vol. 148, pp. 508-515, 2016.

[9] Saepurahman, M. A. Abdullah, and F. K. Chong, "Preparation and characterization of tungsten-loaded titanium dioxide photocatalyst for enhanced dye degradation," *J Hazard Mater*, vol. 176, pp. 451-8, Apr 15 2010.

[10] R. M. Ramli, C. F. Kait, and A. A. Omar, "Photodegradation of aqueous diisopropanolamine using Cu/TiO_2: Effect of calcination temperature and duration," *Applied Mechanics and Materials*, vol. 625, pp. 847-850, 2014.

[11] C. Orha, R. Pode, F. Manea, C. Lazau, and C. Bandas, "Titanium dioxide-modified activated carbon for advanced drinking water treatment," *Process Safety and Environmental Protection*, 2016.

[12] D. Zhang, "Enhanced photocatalytic activity for titanium dioxide by co-modification with copper and iron," *Transition Metal Chemistry*, vol. 35, pp. 933-938, 2010.

[13] W. Zhou, P. Zhang, and W. Liu, "Anatase TiO_2 Nanospindle/ActivatedCarbon (AC) Composite Photocatalystswith Enhanced Activity in Removal ofOrganic Contaminant," *International Journal of Photoenergy*, 2012.

[14] C. B. Ozkal, A. Koruyucu, and S. Meric, "Heterogeneous photocatalytic degradation, mineralization and detoxification of ampicillin under varying pH and incident photon flux conditions," *Desalination and Water Treatment*, vol. 57, pp. 18391-18397, 2016.

[15] A. Zawawi, R. M. Ramli, and N. Y. Harun, "Synergistic Effect Of Adsorption-Photodegradation Of Composite TiO_2/AC For Degradation Of 1-Butyl-3-Methylimidazolium Chloride," *Malaysian Journal of Analytical Sciences*, 2017.

[16] A. Di Paola, E. García-López, G. Marcì, C. Martín, L. Palmisano, V. Rives, *et al.*, "Surface characterisation of metal ions loaded TiO2 photocatalysts: structure–activity relationship," *Applied Catalysis B: Environmental*, vol. 48, pp. 223-233, 2004.

[17] M. G. Alalm, A. Tawfik, and S. Ookawara, "Enhancement of photocatalytic activity of TiO_2 by immobilization on activated carbon for degradation of pharmaceuticals," *Journal of Environmental Chemical Engineering*, vol. 4, pp. 1929–1937, 2016.

[18] A. S. MUHAMMA, J. T. NASER, I. KIRM, and B. Y. JIBRIL, "Photocatalytic Degradation of Methylene Blue and Phenol Using TiO_2/Activated-Carbon Composite Catalysts," *343-348*, vol. 1, p. Asian Journal of Chemistry, 2015.

[19] W.-C. Oh and M.-L. Chen, "Formation of TiO_2 composites on activated carbon modified by nitric acid and their photocatalytic activity," *Journal of Ceramic Processing Research*, vol. 8, p. 316~323, 2007.

[20] X. Wang, Y. Liu, Z. Hu, Y. Chen, W. Liu, and G. Zhao, "Degradation of methyl orange by composite photocatalysts nano-TiO2 immobilized on activated carbons of different porosities," *J Hazard Mater*, vol. 169, pp. 1061-7, Sep 30 2009.

[21] Z. Zhang, Y. Xu, X. Ma, F. Li, D. Liu, Z. Chen, *et al.*, "Microwave degradation of methyl orange dye in aqueous solution in the presence of nano-TiO2-supported activated carbon (supported-TiO2/AC/MW)," *J Hazard Mater*, vol. 209-210, pp. 271-7, Mar 30 2012.

[22] L. Andronic, A. Enesca, C. Cazan, and M. Visa, "TiO2–active carbon composites for wastewater photocatalysis," *Journal of Sol-Gel Science and Technology*, vol. 71, pp. 396-405, 2014.

[23] J. Lemus, C. M. Neves, C. F. Marques, M. G. Freire, J. A. Coutinho, and J. Palomar, "Composition and structural effects on the adsorption of ionic liquids onto activated carbon," *Environmental Science Process Impacts*, vol. 15, pp. 1752-9, 2013.

[24] J. Lemus, J. Palomar, F. Heras, M. A. Gilarranz, and J. J. Rodriguez, "Developing criteria for the recovery of ionic liquids from aqueous phase by adsorption with activated carbon," *Separation and Purification Technology*, vol. 97, pp. 11-19, 2012.

[25] D. Huang, Y. Miyamoto, T. Matsumoto, T. Tojo, T. Fan, J. Ding, *et al.*, "Preparation and characterization of high-surface-area TiO_2/activated carbon by low-temperature impregnation," *Separation and Purification Technology*, vol. 78, pp. 9-15, 2011.

[26] G. Wang, L. Xu, J. Zhang, T. Yin, and D. Han, "Enhanced Photocatalytic Activity of Powders (P25) via Calcination Treatment," *International Journal of Photoenergy*, vol. 2012, pp. 1-9, 2012.

[27] Q. Xiao and L. Ouyang, "Photocatalytic activity and hydroxyl radical formation of carbon-doped TiO2 nanocrystalline: Effect of calcination temperature," *Chemical Engineering Journal*, vol. 148, pp. 248-253, 2009.

[28] P. Górska, A. Zaleska, E. Kowalska, T. Klimczuk, J. W. Sobczak, E. Skwarek, *et al.*, "TiO2 photoactivity in vis and UV light: The influence of calcination temperature and surface properties," *Applied Catalysis B: Environmental*, vol. 84, pp. 440-447, 2008.

[29] S. Obregón, S. W. Lee, and V. Rodríguez-González, "Loading effects of silver nanoparticles on hydrogen photoproduction using a Cu-TiO_2 photocatalyst," *Materials Letters*, vol. 173, pp. 174-177, 2016.

[30] E. M. Siedlecka, W. Mrozik, Z. Kaczynski, and P. Stepnowski, "Degradation of 1-butyl-3-methylimidazolium chloride ionic liquid in a Fenton-like system," *J Hazard Mater*, vol. 154, pp. 893-900, Jun 15 2008.

[31] H. Hassena, "Photocatalytic Degradation of Methylene Blue by Using Al_2O_3/Fe_2O_3 Nano Composite under Visible Light," *Modern Chemistry & Applications*, vol. 176, 2016.

[32] A. F. Alkaim, T. A. Kandiel, F. H. Hussein, R. Dillert, and D. W. Bahnemann, "Enhancing the photocatalytic activity of TiO2 by pH control: a case study for the degradation of EDTA," *Catalysis Science & Technology*, vol. 3, p. 3216, 2013.

[33] U. G. Akpan and B. H. Hameed, "Parameters affecting the photocatalytic degradation of dyes using TiO_2-based photocatalysts: a review," *J Hazard Mater*, vol. 170, pp. 520-9, Oct 30 2009.

[34] Saepurahman, M. A. Abdullah, and F. K. Chong, "Preparation and characterization of tungsten-loaded titanium dioxide photocatalyst for enhanced dye degradation," *Journal of Hazardous Materials*, vol. 176, pp. 451-458, 2010.

[35] C. Andriantsiferana, E. F. Mohamed, and H. Delmas, "Photocatalytic degradation of an azo-dye on TiO_2/activated carbon composite material," *Environmental Technology*, vol. 35, pp. 355-363, 2013.

[36] C. Belver, J. Bedia, M. A. Álvarez-Montero, and J. J. Rodriguez, "Solar photocatalytic purification of water with Ce-doped TiO_2/clay heterostructures," *Catalysis Today*, vol. 266, pp. 36-45, 2016.